

Organization and magnetic properties of cigar-shaped ferrite nanocrystals

A T Ngo and M P Pileni

Université Pierre et Marie Curie, Laboratoire des Matériaux Mésoscopiques et Nanométriques, LM2N, UMR 7070, BP 52, 4 Place Jussieu, 75005 Paris, France
E-mail: ngo@sri.jussieu.fr

New Journal of Physics 4 (2002) 87.1–87.8 (<http://www.njp.org/>)

Received 15 July 2002, in final form 8 October 2002

Published 7 November 2002

Abstract. Cigar-shaped maghemite ($\gamma\text{-Fe}_2\text{O}_3$) nanocrystals dispersed in aqueous solution are subjected to a magnetic field during the deposition (process) on graphite. The nanocrystals can thus be oriented along their long axis to form ribbons at a mesoscopic scale whereas without a field the nanocrystals remain randomly oriented on the substrate. The magnetic properties markedly depend on the organization of the nanocrystals within the mesostructures.

1. Introduction

Ferromagnetic nanomaterials are receiving considerable attention, both theoretically and experimentally, due to their potential in developing high-density magnetic recording media, and to their fascinating experimental behaviour. In these dense systems, the mutual interactions, in particular the dipolar interactions, play an important role. When nanoparticles characterized by superparamagnetic behaviour are agglomerated in dense systems such as granular films, the magnetic properties largely differ both from those of the individual nanocrystals and the bulk material [1]. In our laboratory, collective magnetic properties have been demonstrated when cobalt nanocrystals are self-organized in a 2D hexagonal network. There is an increase in the blocking temperature, and the magnetization curve, when measured with an applied field parallel to the surface of the substrate, is squarer than that obtained for the same nanocrystals isolated in liquid solution. This behaviour is explained in terms of dipolar interactions between adjacent nanocrystals in the self-organized monolayer [2]. The organization induced by an applied magnetic field enables the fabrication of 3D superlattices of ferrite nanocrystals [3, 4]. Collective magnetic properties due to a partial orientation of easy magnetic axes during the deposition were reported [4]. In these cases, the major handicap is that these collective properties were observed at a very low temperature (3 K).

This paper shows that it is possible to align the easy magnetization axes of nanocrystals, at room temperature with a very high reduced remanence.

2. Experimental section

2.1. Products

Iron chloride $\text{Fe}(\text{Cl})_3$, and nitric acid, HNO_3 were from Prolabo. Sodium phosphate, NaH_2PO_4 , sodium citrate, $\text{Na}_3\text{C}_6\text{O}_7\text{H}_5 \cdot 2\text{H}_2\text{O}$ and poly(vinylalcohol), $[-\text{CH}_2\text{CH}(\text{OH})-]_n$ were from Aldrich.

The synthesis of cigar-shaped nanocrystals is described in the appendix. At the end of the synthesis, a neutral magnetic fluid of elongated nanocrystals is obtained.

2.2. Apparatus

A Jeol (100 kV) model JEM 100 CX II transmission electron microscope (TEM) was used to obtain micrographs of the ferrite nanocrystals. The assemblies of these nanocrystals were visualized with a Jeol model JSM-840A scanning electron microscope.

Hysteresis loops at room temperature were determined with a commercial SQUID magnetometer with fields up to $4 \times 10^6 \text{ A m}^{-1}$.

3. Results

Figure 1(a) shows the TEM image obtained by deposition of a drop of solution ($10^{-3}\%$ in mass) on the carbon grid. The average length, width and aspect ratio are ($325 \text{ nm} \pm 17\%$), ($49 \text{ nm} \pm 14\%$) and ($6.7 \pm 14\%$), respectively. The high-resolution TEM (HRTEM) image shows pores aligned with the long axis (e.g. figure 1(b)). Furthermore, the lattice planes are visible over the whole crystal and they have only one orientation. The electron diffraction spots in the measurements of one nanocrystal are indexed to the maghemite structure.

The same drop deposited on the carbon grid in an applied magnetic field of $1.4 \times 10^6 \text{ A m}^{-1}$ shows an orientation of the cigar-shaped nanocrystals with their long axis along the direction of the applied field (e.g. figure 1(c)). However, the amount of material deposited on the carbon grid is too small to measure a magnetic signal. Consequently, fifteen $10 \mu\text{l}$ drops of a solution containing 0.14% in mass of nanocrystals are deposited on the highly oriented pyrolytic graphite (HOPG) substrate. The sample is subjected or not to a magnetic field. The drops remain on the substrate during the evaporation process. By controlling the nanocrystal concentration of the magnetic fluid, the same amount of nanocrystals is deposited on the substrate, making it possible to compare the magnetic behaviour of the various samples.

A thin magnetic film made of cigar-shaped maghemite nanocrystals is obtained by slow evaporation at room temperature. In the absence of a field, the SEM images show, on a large scale, a rather homogeneous film with some cracks (e.g. figure 2(a)). At higher magnification, it is clearly seen that the nanocrystals are randomly oriented (e.g. inset figure 2(a)). The thickness, measured by tilting the sample, varies over $5\text{--}10 \mu\text{m}$ (e.g. figure 2(b)). When a magnetic field ($1.4 \times 10^6 \text{ A m}^{-1}$) is applied during the evaporation in the plane of the substrate, ribbons are formed (e.g. figure 2(c)). At higher magnification (e.g. inset figure 2(c)), it is observed that the cigar-shaped maghemite nanocrystals are mainly oriented along the direction of the applied field.

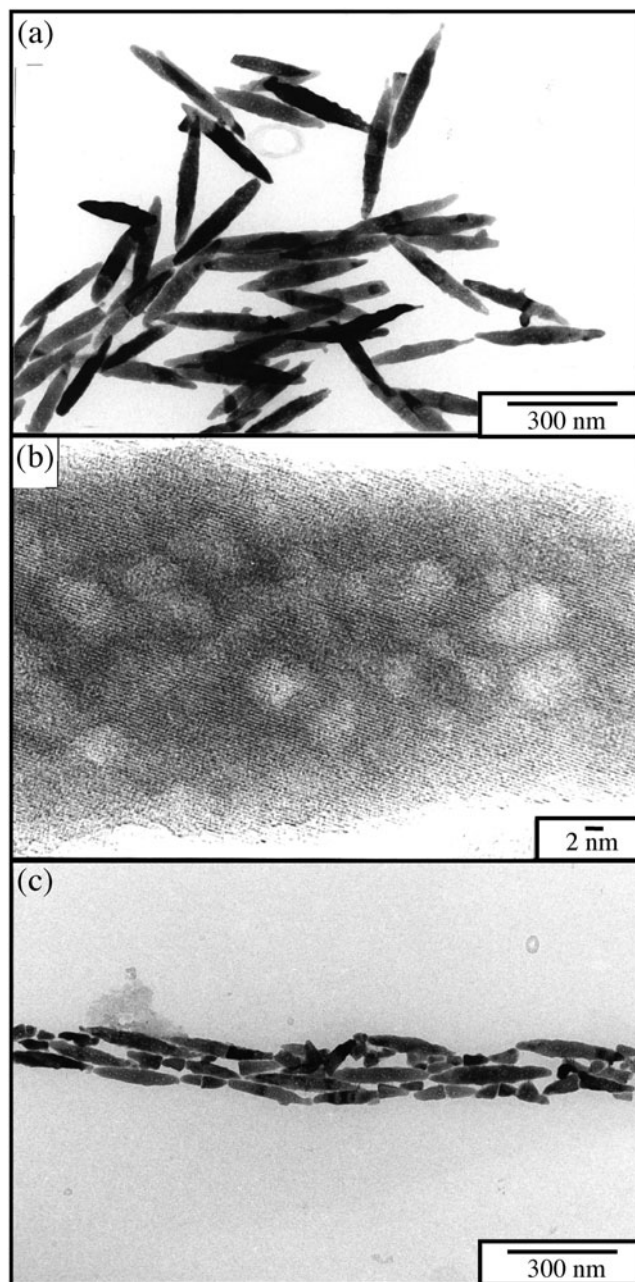


Figure 1. TEM images of cigar-shaped maghemite nanocrystals deposited on a carbon grid (a) in the absence and (c) in the presence of a $1.4 \times 10^6 \text{ A m}^{-1}$ applied field. (b) HRTEM of a cigar-shaped maghemite nanocrystal.

However, some nanocrystals are misaligned from the initial direction of the applied field (see arrows). The thickness of the film remains similar to that obtained in the absence of an applied field (e.g. figure 2(d)).

The magnetic properties of nanocrystals randomly oriented on the HOPG substrate (e.g. figures 2(a) and (b)) are recorded at 290 K with the applied field parallel to the substrate. The magnetization curve (e.g. figure 3) shows a reduced remanence (M_r/M_s) of 0.5. The same

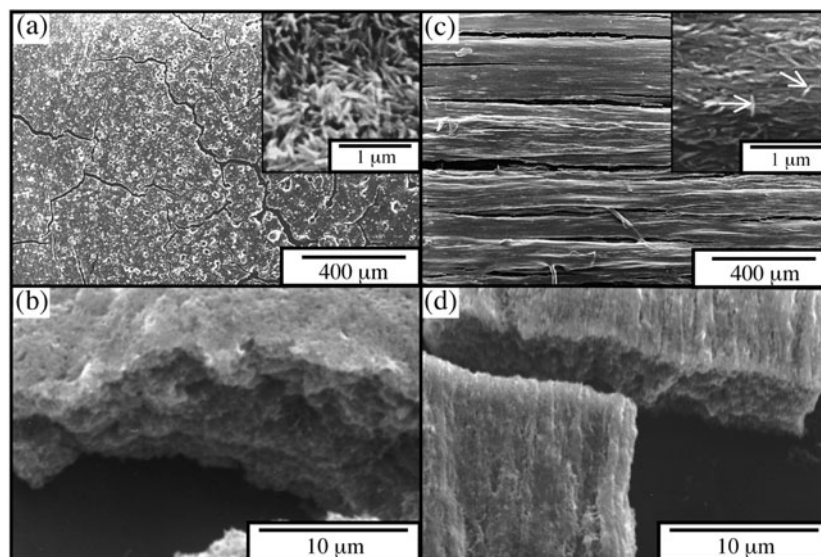


Figure 2. SEM images at various magnifications for cigar-shaped maghemite nanocrystals deposited on HOPG without applied field at zero angle (a) and by 45° tilt (b) and with a non-zero applied field of $1.4 \times 10^6 \text{ A m}^{-1}$ during the deposition process, at zero angle (c) and by 45° tilt (d).

value of the reduced remanence is obtained for nanocrystals dispersed in a polyvinyl alcohol [5] matrix (1% in mass). This value is in good agreement with that expected for an assembly of randomly oriented, single-domain particles with uniaxial anisotropy [6]. Furthermore, according to theoretical calculations by Morrish and Yu [7], elongated $\gamma\text{-Fe}_2\text{O}_3$ particles with an average length below $1.5 \mu\text{m}$ and an aspect ratio of 6.7 are expected to be single-domain. However, in these calculations, the magnetocrystalline anisotropy was neglected with respect to the shape anisotropy. Taking into account the experimental data and the Morrish and Yu [7] calculations, it seems reasonable to conclude that the cigar-shaped maghemite nanocrystals produced in these experiments are single-domain with uniaxial anisotropy. This is consistent with the reduced remanence value (0.5). The coercive field (H_c) is $3.4 \pm 0.08 \times 10^4 \text{ A m}^{-1}$. When the applied magnetic field is perpendicular to the substrate (by turning the substrate plane by 90°), the reduced remanence drops to 0.18 and the coercive field remains quite unchanged ($H_c = 3.2 \pm 0.08 \times 10^4 \text{ A m}^{-1}$).

The magnetization curves (e.g. figure 4) of aligned nanocrystals (e.g. figures 2(c) and (d)) depend on the orientation of the applied magnetic field. When it is parallel to the substrate and parallel to the long axis of the elongated nanocrystals, the hysteresis loop is squarer than that measured when the nanocrystals are randomly oriented on the substrate. The reduced remanence markedly increases ($M_r/M_s = 0.80$) compared to that obtained for a film made of nanocrystals with a random distribution of the easy axes ($M_r/M_s = 0.50$). The coercive field (H_c) is $3.4 \pm 0.08 \times 10^4 \text{ A m}^{-1}$. By applying the magnetic field parallel to the substrate and perpendicular to the nanocrystal alignment, the hysteresis loop is smoother than that obtained when the applied field is parallel to the elongated nanocrystal direction. The reduced remanence and the coercive field drop to 0.24 and $1.8 \pm 0.08 \times 10^4 \text{ A m}^{-1}$, respectively. When the applied field is normal to the substrate, the reduced remanence drops again to 0.11 whereas the coercive field remains unchanged ($H_c = 1.8 \pm 0.08 \times 10^4 \text{ A m}^{-1}$).

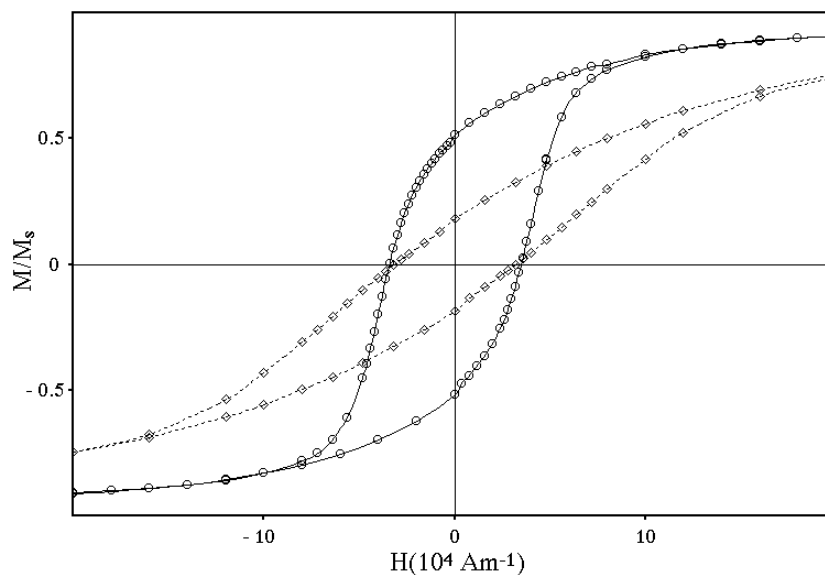


Figure 3. Magnetization curves at 290 K for cigar-shaped maghemite nanocrystals deposited on HOPG without applied field, where the magnetization is recorded with an applied field either parallel (full curves with circles) or normal (dashed curves with squares) to the film made of nanocrystals.

Whatever the applied field direction, saturation magnetization reaches the same value ($M_s = 3.8 \times 10^5 \text{ A m}^{-1}$). This is in good agreement with the value ($M_s = 3.6 \times 10^5 \text{ A m}^{-1}$) measured by Haneda [8].

4. Discussion

The change in the hysteresis loop can be attributed either to the orientation of the easy axes or to the demagnetizing field effects which can be created either by the shape of the nanocrystals or by their dense packing in the thin film. In fact the demagnetizing factor of an isolated prolate spheroid [6, 9], with an aspect ratio of 7, is close to zero when the applied field is parallel to the nanocrystal long axis whereas it is 0.45 along the short axis. Concerning the thin film, the demagnetizing factor is 0 when the applied field is parallel to the plane of the thin film and 1 when it is perpendicular.

When the nanocrystals are randomly dispersed in the film, the change in the hysteresis loop with the orientation of the applied field observed in figure 3 is due to the change in the demagnetizing factor of the film varying from 0 to 1. That of nanocrystals cannot be taken into account because they are randomly dispersed and the average demagnetizing factor remains unchanged (e.g. inset figure 2(a)).

When the nanocrystals are oriented along their long-axis direction and forming ribbons (e.g. figures 2(c) and (d)), several parameters have to be taken into account. Let us first consider the data obtained when the applied field is parallel to the plane of the thin film made of ribbons. In such a case the demagnetizing factor due to the film remains close to zero. The change in the hysteresis loop, when the applied field is either parallel or perpendicular to the nanocrystal long axis, is due to the demagnetizing factor of the nanocrystals themselves and to the orientation

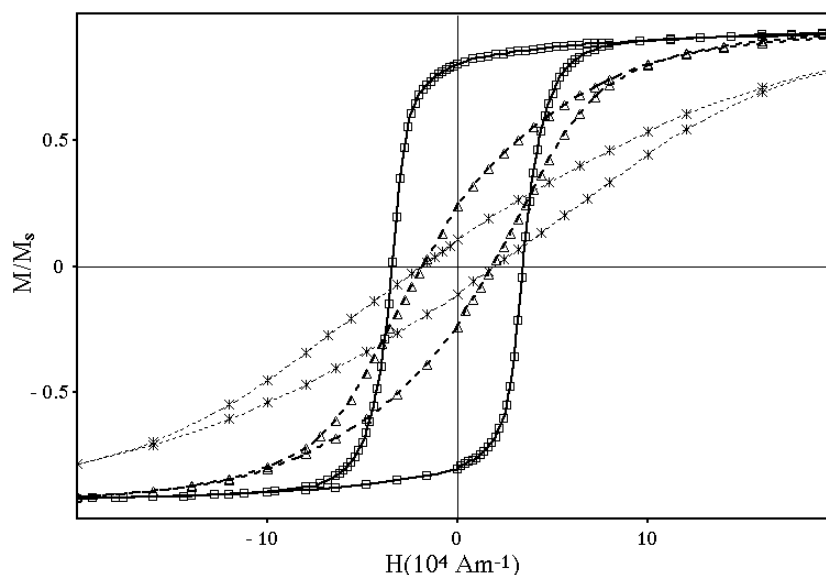


Figure 4. Magnetization curves at 290 K for cigar-shaped maghemite nanocrystals deposited on HOPG with a non-zero applied field of $1.4 \times 10^6 \text{ A m}^{-1}$, where the magnetization is recorded with an applied field either parallel (full curves with squares) or perpendicular (dashed curves with triangles) or normal (dashed curves with asterisks) to the ribbons' direction.

of their easy axes. The form of the nanocrystal creates a shape anisotropy where the easy magnetization axis is parallel to its long axis. This shape anisotropy is the main contribution of the magnetic anisotropy. Therefore, for the assemblies of aligned cigar-shaped nanocrystals with their long axis in the ribbons, a preferential orientation of the easy magnetization axes is expected. Let us assume a total alignment of the easy magnetic axes: the hysteresis loop measured when the applied field is parallel to the easy axes is expected to be rectangular with a reduced remanence of 1. In a perpendicular applied field, no hysteresis loop with zero as reduced remanence is expected [6]. Drops in the reduced remanence (from 0.8 to 0.24) and the coercive field (from $3.4 \pm 0.08 \times 10^4$ to $1.8 \pm 0.08 \times 10^4 \text{ A m}^{-1}$) are observed by changing the orientation of the applied field from parallel to perpendicular to the long axis of the cigar-shaped nanocrystals. Hence, the change in the shape of the magnetization curves with the direction of the applied field is due to the demagnetizing factor of the nanocrystals which leads to a shape anisotropy and to the orientation of the easy axes. Hence, application of a magnetic field during the deposition process enables the rotation of nanocrystals with their long axis along the direction of the applied field. In the figure 2(c) inset, some deviations from complete alignment of nanocrystals are observed. This leads to a distribution of the easy axes with respect to the direction of the ribbons. Let us compare the magnetic parameters such as the reduced remanence and the coercive field of these assemblies of aligned nanocrystals organized in ribbons with those calculated by Stoner and Wohlfarth [6] for an elongated particle whose easy axis makes an angle ψ_0 with the applied field. The reduced remanence obtained for angles between the easy axis and the applied magnetic field of 30° and 40° are 0.86 and 0.76, respectively. The values of the coercive fields for these two angles are roughly constant and close to that of an assembly of particles with randomly oriented easy axes, namely $H_c \approx 0.5H_{cmax}$, where H_{cmax} is the

coercive field for $\psi_0 = 0$. Let us assume that the measured hysteresis loop is an average of the individual loops of the nanocrystals forming the ribbons. Then, this average of the hysteresis loops is approximated by the hysteresis loop of one isolated particle whose easy axis makes an angle ψ_0 with the applied field. We estimate the mean value of the angles of our assembly by fitting both the reduced remanence and the coercive field. Therefore, we obtain $\psi_0 \approx 30^\circ$ for the estimated mean value of the angle of the distribution of the easy axes relative to the direction of the applied field. It is concluded that the drastic increase in the reduced remanence observed in figure 4 is due to the orientation of the easy axes of most of the nanocrystals.

The anisotropy field due to the shape of the nanocrystals is $H_s = (N_b - N_a)M_s$, where N_b and N_a are the demagnetizing factors perpendicular and parallel to the long axis of the particle [6], respectively. The Stoner–Wolfarth model thus predicts that the coercive field is equal to the effective anisotropy field H_a (which comprises both magnetocrystalline and shape anisotropy) when the easy axis is parallel to the applied field. For our cigar-shaped nanocrystals with an aspect ratio of 6.7 and a saturation magnetization $M_s = 3.8 \times 10^5 \text{ A m}^{-1}$, the theoretical value of $H_c = 8 \times 10^4 \text{ A m}^{-1}$ is considerably larger than the observed value of $3.4 \times 10^4 \text{ A m}^{-1}$. This discrepancy can be attributed to particle interactions and surface defects due to the pores observed on the HRTEM image of one nanocrystal (e.g. figure 1(b)). The effective magnetic anisotropy constant, K_{eff} , which includes magnetocrystalline anisotropy and shape anisotropy, is related to the anisotropy field through the following expression: $K_{eff} = H_a M_s/2$. The estimated value of $K_{eff} = 8 \times 10^4 \text{ erg cm}^{-3}$ is larger than the bulk magnetocrystalline anisotropy value, $K_1 = 4.64 \times 10^4 \text{ erg cm}^{-3}$ of $\gamma\text{-Fe}_2\text{O}_3$ [10].

When the applied field is perpendicular to the plane of the sample, i.e. to the thin magnetic film of ribbons, the reduced remanence drops to 0.11. In such a case the applied field is always perpendicular to the ribbon direction and parallel to the short axis of the cigar-shaped nanocrystals. Thus, the demagnetizing factor of the individual nanocrystals remains unchanged and the change in the hysteresis loop is only due to the change in the demagnetizing factor of the thin magnetic film.

5. Conclusion

In this paper it is demonstrated that a thin magnetic film is obtained by a slow evaporation on a substrate of a ferrofluid made of cigar-shaped $\gamma\text{-Fe}_2\text{O}_3$ nanocrystals. Application of an external magnetic field during the evaporation changes the structure of the film at the mesoscopic scale. The nanocrystals are assembled in ribbons. The reduced remanence measured with a field parallel to the ribbons ($M_r/M_s = 0.80$) drastically increases compared to that measured with a field perpendicular to the ribbons' direction ($M_r/M_s = 0.24$). Similarly, the coercive field when the field is perpendicular is half that obtained when the field is parallel to the ribbons. This means that the cigar-shaped nanocrystals are partially aligned in the ribbons' direction. The angle between the easy magnetization axes and the applied field can be reduced to a mean value of 30° . Furthermore, from the magnetization measurements with the applied field normal to these films, the reduced remanence markedly decreases. This clearly indicates a strong effect of the demagnetizing field perpendicular to the film surface. Similar behaviour was observed in our previous work with maghemite spherical nanocrystals [4]. However, the major difference between these two results is the temperature at which the process takes place. With spherical nanocrystals, such behaviour was observed at 3 K, whereas it is now observed at room temperature.

Acknowledgments

We thank Drs Vincent Russier and Johannes Richardi, of our laboratory, for very fruitful discussions. Thanks are also due to Dr A Kahn-Harari of the CNRS UMR 7574 of the ENSCP of Paris, for providing the conversion of α -Fe₂O₃ to γ -Fe₂O₃ nanocrystals. We are grateful to Dr G Lebras and E Vincent of the Service de Physique de l'Etat Condensé (Saclay) for their help with the SQUID measurements.

Appendix

Making slight changes in the well known synthesis described by Matijevic [11] produced elongated maghemite nanocrystals. An aqueous solution of iron (III) chloride, [FeCl₃] = 2×10^{-2} M, and sodium phosphate, [NaH₂PO₄] = 4.5×10^{-4} M, is heated at 100 °C for 48 h. This is centrifuged, a precipitate appears, the supernatant removed and the nanocrystals are dispersed again in water. At this stage, the nanocrystals produced are hematite (α -Fe₂O₃). This procedure is repeated until the supernatant is optically clear without any remaining salts. Water is removed from the solution and the powder is dried in an air oven at 70 °C for 24 h. The dried powder is then annealed in a furnace at 360 °C under a continuous hydrogen gas flow to transform hematite nanocrystals into magnetite (Fe₃O₄). After 3 h, the hydrogen flow is turned off and the powder exposed to air. The furnace temperature is decreased to 240 °C over 2 h in order to reoxidize the magnetite nanocrystals into maghemite (γ -Fe₂O₃). The powder is redispersed in aqueous 10^{-2} M HNO₃. Sodium citrate, [Na₃C₆O₇H₅] = 1.5×10^{-2} M, is added to the solution, which is stirred for 30 min at 90 °C, and the nanocrystals precipitate on addition of acetone. After washing with a large excess of acetone, the powder is dried in air and the particles coated with citrate ions are dispersed in an aqueous solution.

References

- [1] Chien C L 1991 *J. Appl. Phys.* **69** 5267
- [2] Russier V, Petit C, Legrand J and Pileni M P 2000 *Phys. Rev. B* **62** 3910
- [3] Ngo A T and Pileni M P 2000 *Adv. Mat.* **12** 276
- [4] Ngo A T and Pileni M P 2001 *J. Phys. Chem. B* **105** 53
- [5] Ngo A T, Bonville P and Pileni M P 1999 *Eur. Phys. J. B* **9** 583
- [6] Stoner E C and Wohlfarth E P 1948 *Phil. Trans. R. Soc. A* **240** 559
Reprinted in 1991 *IEEE. Trans. Magn.* **27** 3475
- [7] Morrish A H and Yu S P 1955 *J. Appl. Phys.* **26** 1049
- [8] Haneda K and Morrish A H 1980 *IEEE Trans. Magn.* **16** 50
- [9] Osborn J A 1945 *Phys. Rev.* **67** 351
- [10] Bate G 1975 *Magnetic Oxides* ed D J Craik (London: Wiley) p 689
- [11] Ozaki M and Matijevic E 1985 *J. Colloid Interface Sci.* **107** 199